Two-cell interactions in autologous chemotaxis

Aditya S. Khair [*]

Department of Chemical Engineering, Carnegie Mellon University, Pittsburgh Pennsylvania 15213, USA

An advection-diffusion-reaction model for autologous chemotaxis of two cells in an interstitial flow is analyzed. Each cell secretes ligands uniformly over its surface; the ligands are absorbed by surface receptors anisotropically due to the flow and interaction between ligand fields around each cell. The absorption is quantified in terms of a vectorial anisotropy parameter, A, which is proportional to the first moment of the ligand concentration field about the surface of each cell. We consider the physiologically relevant limit of a weak interstitial flow, where the Péclet number, Pe, which characterizes the relative importance of ligand transport via advection to diffusion, is small. We further assume that the cells are separated at a distance that is large compared to the sum of their radii. These conditions allow us to utilize a reciprocal theorem and the method of reflections to construct an asymptotic approximation for A to first order in Pe for widely separated cells. We find that interactions between the cells: (i) reduce the flow-aligned ligand anisotropy around each cell and (ii) lead to a component of A that is perpendicular to the flow direction. The interaction is long ranged, decaying with the inverse distance between cells to leading order. We finally discuss how interactions between multiple cells could affect our findings.

I. INTRODUCTION

Autologous chemotaxis (AC) refers to the migration of a cell due to small molecules, or ligands, that the cell secretes and subsequently detects via surface receptors. Spatial symmetry breaking is a necessary feature of this autocrine signaling mechanism: A cell is supposed to secrete ligands uniformly over its surface and, in contrast, detect them nonuniformly, thereby garnering information about the anisotropy of its environment. Said information is used by the machinery of the cell to direct migration. The pioneering studies of Swartz and co-workers demonstrated that interstitial flow in the extracellular matrix provides the key symmetry breaking for AC [1,2]. Specifically, interstitial flow drives advective flux of secreted ligands that breaks the fore-aft symmetry of their concentration field around a cell [3–6]. This asymmetry is detected by the cell as an anisotropic flux to its surface receptors. Hence, the cell senses the directionality of the interstitial flow and can migrate accordingly. AC guided by interstitial flow due to lymphatic drainage has been implicated as a driver for cancer metastasis, where cells traffic from a primary tumor to other body parts [7,8]. Experiments have shown AC of breast cancer and melanoma cells [2,9], glioblastoma cells [10,11], and endothelial cells [12].

Recently, Fancher *et al.* [13] proposed and analyzed an advection-diffusion-reaction transport model for AC of a single cell, focusing on the sensory precision of absorption and reversible binding models for ligand detection. Those authors also note that cells do not undergo AC in isolation, however. Indeed, more generally, multicellular sensing is acknowledged to be relevant in the collective migration of groups of cells exposed to chemoattractant gradients [14–18]. Specifically, AC of cancer cells can be promoted by adjacent fibroblast cells [19]. Further, migration depends on cell seeding density: At sufficiently high density the direction of cancer cell migration can even reverse from downstream to upstream of the interstitial flow. In this case, a mechanical pressure-sensing mechanism is claimed to be the dominant driver for migration, suggesting that AC is inhibited at larger seeding density [9]. In particular, neighboring cells induce paracrine signaling cues, since the distribution of a secreted ligand around one cell affects the distribution around other cells. The goal of the present work is to quantify how such interaction between cells affects AC. To this end, we analyze a minimal mathematical model, in the spirit of Ref. [13], for advection-diffusion-reaction transport of a secreted ligand between neighboring cells in an interstitial flow. Examining the interaction between two cells is a natural extension to the analysis of [13]. As we will show below, in this case one can still obtain analytical results for the ligand anisotropy around each cell, which furthers understanding of how cell interactions affect AC. Our main predictions are that interaction between cells (i) reduces the flow-aligned ligand anisotropy around each cell and (ii) leads to a component of the anisotropy that is perpendicular to the flow direction. Moreover, the interaction is long ranged: The influence of a cell on the anisotropy of the ligand field around a neighbor decays as the inverse of the center-to-center distance between the pair.

II. MODEL DEVELOPMENT

Consider two identical, spherical cells of radii a^* with center-to-center separation vector d^* (Fig. 1). Here, and on-

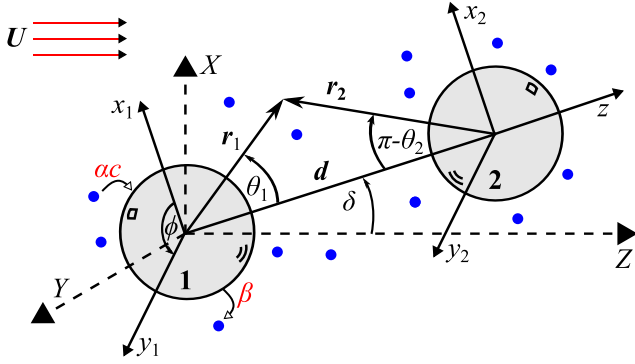---

*akhair@andrew.cmu.edu

024404-1

FIG. 1. Definition sketch for interaction between two cells (labelled "1" and "2") undergoing AC in an interstitial flow. The cells are separated by vector $\boldsymbol{d}$, which makes an angle δ with the ambient free stream $\boldsymbol{U}$. Cells secrete ligand uniformly at rate β and absorb ligand at rate αc, where c is the ligand concentration field and α is the absorption velocity.

ward, dimensional variables will be decorated with an asterisk superscript. The cells are immersed in an interstitial flow that approaches a uniform stream $\boldsymbol{U}^*$ at large distances from each cell. Let c^* denote the number density, or concentration, field of ligand exterior to each cell, which at steady state is governed by the advection-diffusion transport equation $\boldsymbol{v}^* \cdot \nabla^* c^* = D^* \nabla^{*2} c^*$. Here D^* is the diffusion coefficient of a ligand, and $\boldsymbol{v}^*$ is the incompressible ($\nabla^* \cdot \boldsymbol{v}^* = 0$) fluid velocity field. Interstitial flows in the extracellular matrix are commonly modeled using the Brinkman equation [20] for porous media [1,5], which approximates the effect of obstacles in the matrix as a distributed resistance, or damping force, on the flow. The Brinkman equation reads $\mu^* \nabla^{*2} \boldsymbol{v}^* - \nabla^* p^* = \mu^* \kappa^{*2} \boldsymbol{v}^*$, where p^* is the dynamic pressure, μ^* is the fluid viscosity, and $1/\kappa^*$ is a screening length at which viscous and damping forces balance. We assume that ligands are secreted from each cell surface uniformly at a rate β^* per unit area. Ligands are then absorbed by receptors via a first-order reaction with local flux $\alpha^* c^*$, where α^* is the absorption rate with units of length per time. Thus, at each cell surface there is a flux balance $-D^* \boldsymbol{n} \cdot \nabla^* c^* = \beta^* - \alpha^* c^*$, where $\boldsymbol{n}$ is the outward unit normal to the surface. This boundary condition assumes that fluid cannot penetrate or deform the cell, $\boldsymbol{v}^* \cdot \boldsymbol{n} = 0$. The concentration attenuates, $c^* \to 0$, far from each cell. Our central goal is to calculate the anisotropy of the absorption flux over the surface of each cell, accounting for interstitial flow and interaction between the cells. To that end, we define a vectorial anisotropy order parameter $\boldsymbol{A}^* = (4\pi a^{*2})^{-1} \int \alpha^* c^* \boldsymbol{n} \, dS^*$, where dS^* is an element of solid angle over the cell surface. Clearly, $\boldsymbol{A}^* = 0$ if the flux is uniform. The values of $\boldsymbol{A}^*$ for each cell are equal since the cells are identical.

The problem is rendered dimensionless by normalizing distance by a^*, concentration by $1/a^{*3}$, velocity by $U^* = |\boldsymbol{U}^*|$, and pressure by an as-yet-undetermined scale P^*. The dimensionless advection-diffusion equation is $\mathrm{Pe}\boldsymbol{v} \cdot \nabla c = \nabla^2 c$, in which, and henceforth, the lack of an asterisk superscript indicates a dimensionless quantity, e.g., the dimensionless concentration $c = c^* a^{*3}$ and dimensionless velocity $\boldsymbol{v} = \boldsymbol{v}^*/U^*$. Here $\mathrm{Pe} = U^* a^*/D^*$ is a Péclet number that characterizes the importance of advection versus diffusion in

establishing the concentration field. Interstitial flow speeds due to lymphatic drainage are around 1 μm/s [21,22], which for a cell of $a^* = 10 \, \mu$m and $D^* = 100 \, \mu$m²/s [1] yields $\mathrm{Pe} = O(0.1)$. Hence, Pe is typically small. The dimensionless Brinkmann equation reads $\nabla^2 \boldsymbol{v} - (a^* P^*/\mu^* U^*)\nabla p = \delta^2 \boldsymbol{v}$, where $p = p^*/P^*$ is a normalized pressure and $\delta = (\kappa^* a^*)^2$. The dimensionless boundary conditions at the cell surfaces are $-\boldsymbol{n} \cdot \nabla c = \beta - \alpha c$, where $\beta = \beta^* a^{*4}/D^*$ is a normalized secretion rate, and $\alpha = \alpha^* a^*/D^*$ is a normalized absorption rate or Damkohler number. A secretion rate of 1000 ligands per hour [13] yields $\beta = O(10^{-2})$. Thus, the dimensionless anisotropy parameter $\boldsymbol{A} = A^* a^{*3}/\alpha^* = (4\pi)^{-1} \int c\boldsymbol{n} \, dS$ is a function of five dimensionless groups: α, β, δ, Pe, and, finally, the normalized separation distance $d = |\boldsymbol{d}^*|/a^*$.

III. RESULTS

The advection-diffusion equation cannot be solved exactly due to the complexity of the two-sphere geometry, which generally yields a concentration field that varies in three spatial dimensions. The exception is when the separation vector between the cells is aligned with the ambient flow: In this case, the concentration is axially symmetric about $\boldsymbol{d}^*$. Here we invoke physically realistic simplifying assumptions to ultimately obtain an asymptotic, closed-form, approximation to the anisotropy order parameter. First, the permeability in the extracellular matrix is sufficiently low that $\delta = O(10^3)$ [2,13]. This means that the viscous stresses in Brinkman's equation can be dropped: The resulting flow is described by Darcy's law, $\nabla p = \boldsymbol{v}$, with pressure scale $P^* = \delta\mu^* U^* \kappa^*$ chosen to balance damping. Using the continuity equation and no-penetration condition at the cell surface, it is seen that the resulting velocity field is the same as in irrotational flow, with p playing the role of velocity potential. This implies that the tangential component of the velocity field does not vanish at the cell surface, which is expected to lead to an overestimation of $\boldsymbol{A}$, since the flow can more easily advect ligands adjacent to the surface. Second, we assume that the cells are widely separated, $d \gg 1$. This will enable us to calculate interactions between their concentration fields via the method of reflections [23–26]. Third, in accordance with physiological and *in vitro* conditions, we assume that Pe is small. One might think this to imply that advection is a weak perturbation to the purely diffusive (Pe = 0) concentration field. However, the limit Pe $\to 0$ is singular for advection-diffusion problems in unbounded flows [27,28]. Specifically, even though Pe is small, advection is as important as diffusion at large distances from each cell, $r = |\boldsymbol{r}| = O(1/\mathrm{Pe})$, where $\boldsymbol{r}$ is the position vector from the center of a cell. Physically, the ligand concentration field is primarily dictated by diffusion at a distance $r = O(1)$ from a cell, with an algebraic decay like $1/r$ for a cell that is a net source of ligand. However, at $r = O(1/\mathrm{Pe})$ the concentration field is "screened" by advection with the imposed flow, such that it decays exponentially with increasing distance. (This exponential decay occurs almost everywhere: The exception is a thin wake region downstream of the cell, where the algebraic $1/r$ decay persists.) Matched asymptotic expansions are needed to construct perturbative solutions at small Pe, where the concentration field has separate expansions in inner [$r = O(1)$] and outer [$r = O(1/\mathrm{Pe})$]

regions. This approach was used in Ref. [13] to evaluate the equivalent of our anisotropy parameter A through $O(\text{Pe})$ for an isolated spherical cell. In particular, those authors determined the first, $O(\text{Pe})$, advective contribution to the concentration field in the inner region, which possesses the requisite fore-aft asymmetry for a nonzero anisotropy parameter. It is unclear how to extend their analysis to two (or more) cells: Aside from the forbidding algebra, there is a conceptual issue of whether the separation distance between cells is such that one cell sits in the outer or inner region of the concentration field of the other.

Therefore, to analyze the coupled influence of two-cell interactions and interstitial flow on AC we adopt a different strategy. We will construct an integral relation, based on the reciprocal theorem in transport phenomena [29], which allows calculation of A through $O(\text{Pe})$ using only the purely diffusive ($\text{Pe} = 0$) concentration field. To begin, we consider a single cell in a background ligand field c^∞. Ultimately, c^∞ will represent the field due to a second cell. Let $c' = c - c^\infty$ denote the disturbance from the background due to a cell at $r = 0$. This disturbance satisfies $\text{Pe}\,\boldsymbol{v} \cdot \nabla c' = \nabla^2 c'$, subject to $c' \to 0$ as $r \to \infty$, and $\boldsymbol{n} \cdot \nabla c' - \alpha c' = -(\boldsymbol{n} \cdot \nabla c^\infty - \alpha c^\infty) - \beta$ at $r = 1$. Let $\tilde{c}$ denote the concentration belonging to an "auxiliary problem" that satisfies Laplace's equation, $\nabla^2 \tilde{c} = 0$, around the cell. Evidently, there is an integral relation between the disturbance and auxiliary fields,

$$\int \tilde{c}(\boldsymbol{v} \cdot \nabla c' - \nabla^2 c') \, dV + \int c' \nabla^2 \tilde{c} \, dV = 0, \qquad (1)$$

where dV is a volume element of fluid exterior to the cell. Equation (1) leads to the following expression for the anisotropy order parameter (see Appendix):

$$
\begin{aligned}
\left(1 + \frac{\alpha}{2}\right)\boldsymbol{A} &= \frac{1}{2}\nabla c^\infty|_{r=0} + \frac{5\text{Pe}}{60}\nabla(\boldsymbol{v} \cdot \nabla c^\infty)|_{r=0} \\
&\quad + \frac{\text{Pe}}{8\pi}\int (c - c^\infty)\boldsymbol{v} \cdot \nabla\left(\frac{\boldsymbol{r}}{r^3}\right) dV \\
&\quad + O(\text{Pe}^2).
\end{aligned} \qquad (2)
$$

First consider an isolated cell in a ligand-free background, $c^\infty = 0$. The irrotational velocity field is

$$\boldsymbol{v} = \boldsymbol{U} + \frac{1}{2r^3}\boldsymbol{U} \cdot \left(\boldsymbol{I} - \frac{3\boldsymbol{rr}}{r^2}\right), \qquad (3)$$

where $\boldsymbol{U}$ is a unit vector along the free stream and $\boldsymbol{I}$ is the identity tensor. At $\text{Pe} = 0$ the cell acts as an isotropic source, or monopole, with ligand concentration field $c = \gamma/r$, where $\gamma = \beta/(1 + \alpha)$ represents the monopole strength. Inserting this field and (3) into (2) yields (see Appendix)

$$\boldsymbol{A} = \frac{\gamma \boldsymbol{U}}{4(2 + \alpha)}\text{Pe} + o(\text{Pe}) \text{ as } \text{Pe} \to 0. \qquad (4)$$

This result is in agreement with Eq. (7) of Ref. [13]: Our assumption of Darcy flow corresponds to $w = 2$ in their notation and their scalar anisotropy factor A is normalized by the average concentration over the cell surface, which requires dividing (4) by γ. We reemphasize that in Ref. [13] the $O(\text{Pe})$ contribution to the anisotropy parameter was obtained by solving for the inner concentration field through $O(\text{Pe})$; in

contrast, our use of the reciprocal theorem (2) only requires the diffusive ($\text{Pe} = 0$) concentration field around the cell. Physically, Eq. (4) implies that the ligand concentration is polarized along the direction of the interstitial flow, in proportion to the flow strength; the polarization, or anisotropy, increases linearly with the secretion rate, β; and the anisotropy decreases with increasing absorption rate, α. This last behavior arises as increasing α reduces the time that a secreted ligand can be advected along flow streamlines before it is absorbed by the cell.

We now analyze interaction between two cells in an interstitial flow. The ambient flow $\boldsymbol{U}$ is taken along the Z axis of a Cartesian frame (X, Y, Z). The two cells are labeled "1" and "2." Let (x, y, z) be a particle-fixed Cartesian system with origin at the centroid of cell 1: the z axis passes through the line of centers of the two cells and is at an angle δ to the Z axis, and the y axis is taken as normal to the plane of $\boldsymbol{U}$. Thus, $\boldsymbol{U} = \cos\delta\boldsymbol{e}_z - \sin\delta\boldsymbol{e}_x$, where $\boldsymbol{e}_z$ and $\boldsymbol{e}_x$ are unit vectors along the z and x axes, respectively. Spherical polar coordinate systems (r_1, θ_1, ϕ) and (r_2, θ_2, ϕ) attached to the centers of cells 1 and 2, respectively, are also introduced. Here ϕ is the common azimuthal angle in the xy plane, and the polar angles θ_1 and θ_2 are measured counterclockwise from the z axis. The two-cell configuration is thus specified by the angle γ and center-to-center separation distance d (Fig. 1). To a first approximation at large d the ligand concentration at $\text{Pe} = 0$ is a superposition of the sources due to each cell in isolation: $c \sim c^{(1)} + c^{(2)}$ as $d \to \infty$, where $c^{(i)} = \gamma/r_i$. Thus, the ligand field due to cell 1 appears to cell 2 as a uniform background at leading order, $c^{(1)} = \gamma/d + O(1/d^2)$. Cell 2 responds to this paracrine signal by generating a harmonic first reflection, $c^{(21)}$, say, to satisfy the flux condition at its surface, $\partial c^{(21)}/\partial r_1 - \alpha c^{(21)} = -(\partial c^{(1)}/\partial r_1 - \alpha c^{(1)})$. A simple calculation shows that $c^{(21)} = -\gamma\alpha/[(1 + \alpha)dr_2] + O(d^{-2})$. Hence, the disturbance field around cell 2 is $c - c^\infty \sim \gamma\{1 - \alpha/[d(1 + \alpha)]\}(1/r_2) + O(1/d^2)$. Inserting this expression into (2) yields

$$\boldsymbol{A} \sim \frac{\gamma \boldsymbol{U}}{4(2 + \alpha)}\left[1 - \frac{\alpha}{1 + \alpha}\frac{1}{d} + o\left(\frac{1}{d}\right)\right]\text{Pe} \qquad (5)$$

as $\text{Pe} \to 0$, which shows that the interaction reduces the anisotropy parameter, since the $O(1/d)$ contribution is negative. This occurs as cell 1 acts a uniform source of ligand for cell 2 (and vice versa), which results in a reduced anisotropy of the absorption flux around each cell: This finding is in agreement with finite element simulations of Ref. [9]. The uniformity also means that A is collinear with $\boldsymbol{U}$. The interaction is notably long ranged, decaying as $1/d$.

The method of reflections can be continued to yield the improved estimate (see Appendix)

$$
\begin{aligned}
\left(1 + \frac{\alpha}{2}\right)\boldsymbol{A} &= \frac{\gamma \boldsymbol{U}\text{Pe}}{8}\left[1 - \frac{\alpha}{1 + \alpha}\frac{1}{d}\right] \\
&\quad - \frac{\gamma \boldsymbol{d}}{2d^3} - \frac{\gamma\text{Pe}\boldsymbol{U}}{12} \cdot \left(\frac{\boldsymbol{I}}{d^3} - 3\frac{\boldsymbol{dd}}{d^5}\right) \\
&\quad + \frac{\gamma\text{Pe}}{8d^3}\left[\frac{\alpha - 2}{7(3 + \alpha)}\boldsymbol{U} \cdot \left(\boldsymbol{I} + \frac{\boldsymbol{dd}}{d^2}\right) - \frac{\alpha^3}{(1 + \alpha)^3}\boldsymbol{U}\right] \\
&\quad + o(\text{Pe}\,d^{-3}).
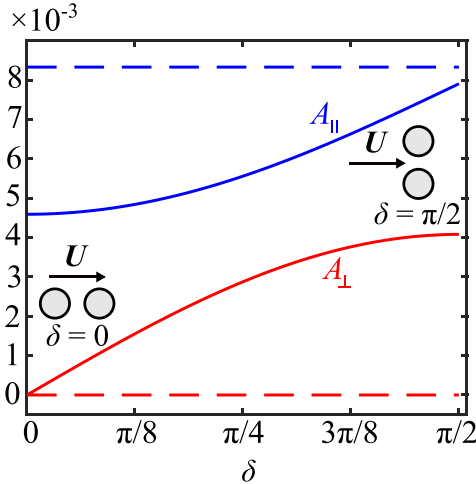\end{aligned} \qquad (6)
$$

FIG. 2. Parallel $A_\parallel$ and perpendicular $A_\perp$ components of anisotropy order parameter $\boldsymbol{A}$. Here Pe = 0.1, $d = 10$, and $\alpha = \gamma = 1$. The dashed lines indicate the values of $A_\parallel$ and $A_\perp$ for an isolated cell.

The first line of (6) is the isolated cell and first reflection contributions to $\boldsymbol{A}$ (5). The remaining terms complete $\boldsymbol{A}$ through $O(\text{Pe}d^{-3})$: They arise from higher-order contributions to the first reflection and multiple reflections between the cells. Notably, the anisotropy parameter is now not solely along the direction of the free stream: $\boldsymbol{A}$ even has components perpendicular to $\boldsymbol{U}$. This misalignment suggests that the paracrine signaling due to intercellular interaction interferes with the interstitial flow aligned anisotropy due to autocrine signaling of an isolated cell. This behavior is illustrated in Fig. 2 by plotting the parallel, $A_\parallel = \boldsymbol{A} \cdot \boldsymbol{U}$, and perpendicular, $A_\perp = |\boldsymbol{A} \cdot (\boldsymbol{I} - \boldsymbol{U}\boldsymbol{U})|$, components of the anisotropy vector as a function of δ. Here $A_\parallel$ monotonically increases with δ, such that the maximum flow-aligned anisotropy is when the cells are perpendicular to the flow, $\delta = \pi/2$. However, this increase is accompanied by an increased misaligned anisotropy $A_\perp$, which also monotonically increases with δ. This highlights a delicate interplay of intercellular interaction and interstitial flow in AC.

IV. CONCLUSIONS

We have predicted that two-cell interactions affect AC via (i) reduction of the flow-aligned ligand anisotropy around each cell and (ii) generation of a component of $\boldsymbol{A}$ that is perpendicular to the flow direction. Our work highlights that AC involves autocrine and paracrine signaling, the latter driven by interactions of the ligand fields between neighboring cells. We have deliberately used the simplest model of ligand transport to emphasize the importance of interactions between cells. For instance, we ignored any mechanical effects of interstitial flow on cell migration, which have been considered in multiphase models of AC [30–32]. Further, one could consider more sophisticated models of ligand-receptor binding, or multiple ligand species, some of which are released from the extracellular matrix rather than secreted from the cells. Here note that the reversible binding model in Ref. [13] corresponds, at steady state, to the small-α limit of our absorption model. It would also be interesting to extend our calculations to

closer separations, using twin multipole expansions [33] or bispherical coordinates [34]. Further, our reciprocal-theorem approach can readily be adapted to analyze nonuniform receptor coverage or nonspherical cells. An important direction is to go beyond two-cell interactions and consider AC of multiple cells. Recall that interstitial flow screens the ligand concentration field due to single cell at a (dimensional) distance $l_a^* = a^*\text{Pe}^{-1}$ at small Pe. Next, consider a suspension of cells, with small cell volume fraction $s = \frac{4\pi}{3}n^*a^{*3}$ where n^* is the cell number density, secreting ligand at Pe = 0. The ligand concentration field due to a "reference" cell in the suspension is screened by the other cells over a length $l_s^* = a^*s^{-1/2}$. This screening occurs as the other cells also secrete ligand, thereby effectively consuming the concentration field due to the reference cell. Consequently, the ligand field due to the reference cell decays exponentially with distance beyond l_s^*, as opposed to the algebraic ($1/r$) decay for an isolated cell at Pe = 0. The present analysis applies when screening due to the interstitial flow dominates over screening by the suspension, which requires that the ratio of screening lengths $l_a^*/l_s^* < 1$, or in dimensionless terms $\text{Pe}/s^{1/2} > 1$. Using the definition of s, this translates into the requirement that the cell density $n^* < (3/4\pi)U^{*2}/a^*D^{*2} = (3/4\pi)\text{Pe}^2/a^{*3}$ for our analysis to be relevant for multiple cells. As an example, taking $a^* = 10$ μm and Pe = 0.1 yields $n^* < 2.4 \times 10^6$ cells/ml. For $l_a^*/l_s^* > 1$ screening by the suspension dominates: Here the ligand secretion by the cells in the suspension effectively smears out the polarization of the ligand distribution around a reference cell due to the interstitial flow, suggesting that the latter has a relatively minor affect. This may be related to the finding of Ref. [9] that AC is less important at high cell density. For $l_a^* \sim l_s^*$ the anisotropy parameter will have a coupled dependence on the cell volume fraction (s) and interstitial flow (Pe), in analogy to problems of heat and mass transfer in fixed beds [35,36]. We will, however, leave a more detailed analysis of AC for multiple cells to a future study.

APPENDIX

1. Derivation of Eq. (2)

Here we derive Eq. (2). Our starting point is Eq. (1), in which c' is the disturbance concentration due to a cell at the origin ($r = 0$) in a background field c^∞ and $\tilde{c}$ is an auxiliary concentration field. The latter satisfies Laplace's equation, $\nabla^2\tilde{c} = 0$. We choose the auxiliary field to obey the Neumann condition $\boldsymbol{n} \cdot \nabla\tilde{c} = \boldsymbol{U} \cdot \boldsymbol{n}$ at the cell surface $r = 1$ and attenuate as $r \to \infty$. It is readily shown that

$$\tilde{c} = -\frac{1}{2}\frac{\boldsymbol{U} \cdot \boldsymbol{r}}{r^3}. \tag{A1}$$

Inserting (A1) into (1) and using the constancy of $\boldsymbol{U}$ leads to

$$\int c'\boldsymbol{n}\,dS = -\frac{1}{2}\int (\boldsymbol{n} \cdot \nabla c')\boldsymbol{n}\,dS$$
$$-\frac{1}{2}\int (\text{Pe}\boldsymbol{v} \cdot \nabla c')\left(\frac{\boldsymbol{r}}{r^3}\right)dV. \tag{A2}$$

The continuity equation, $\nabla \cdot \boldsymbol{v} = 0$, and no-penetration condition, $\boldsymbol{n} \cdot \boldsymbol{v} = 0$ at $r = 1$, are used to manipulate the second integral on the right-hand side of (A2) as

$$\int \left(\boldsymbol{v} \cdot \nabla c' \right) \left(\frac{\boldsymbol{r}}{r^3} \right) dV = -\int c' \boldsymbol{v} \cdot \nabla \left(\frac{\boldsymbol{r}}{r^3} \right) dV. \quad (A3)$$

Now, at $r = 1$, we have the flux condition

$$\boldsymbol{n} \cdot \nabla c' = \alpha c' - \beta - (\boldsymbol{n} \cdot \nabla c^\infty - \alpha c^\infty). \quad (A4)$$

Substituting (A3) and (A4) into (A2) yields

$$\left(1 + \frac{\alpha}{2} \right) \int c\boldsymbol{n} \, dS = \int c^\infty \boldsymbol{n} \, dS + \frac{1}{2} \int (\boldsymbol{n} \cdot \nabla c^\infty) \boldsymbol{n} \, dS$$
$$+ \frac{\text{Pe}}{2} \int (c - c') \boldsymbol{v} \cdot \nabla \left(\frac{\boldsymbol{r}}{r^3} \right) dV. \quad (A5)$$

In deriving (A5) we have used the uniformity of the secretion rate β over the surface, which implies $\int \beta \boldsymbol{n} \, dS = 0$. The background concentration is now expanded in a Taylor series about the center of the particle,

$$c^\infty(\boldsymbol{r}) = c^\infty|_{r=0} + \boldsymbol{r} \cdot \nabla c^\infty|_{r=0} + \tfrac{1}{2} \boldsymbol{r}\boldsymbol{r} : \nabla\nabla c^\infty|_{r=0}$$
$$+ \tfrac{1}{6} \boldsymbol{r}\boldsymbol{r}\boldsymbol{r} \vdots \nabla\nabla\nabla c^\infty|_{r=0} + \cdots. \quad (A6)$$

Therefore, we have

$$\int \boldsymbol{n} c^\infty \, dS = \frac{4\pi}{3} \nabla c^\infty|_{r=0} + \frac{4\pi}{30} \nabla \nabla^2 c^\infty|_{r=0}$$
$$+ O(\nabla \nabla^4 c^\infty|_{r=0}). \quad (A7)$$

The second term on the right-hand side of (A7) is rewritten using the advection-diffusion equation, $\nabla^2 c^\infty = \text{Pe}\boldsymbol{v} \cdot \nabla c^\infty$. Therefore, the third term on the right-hand side of (A7) becomes $\nabla \nabla^4 c^\infty = \text{Pe}\nabla \nabla^2 (\boldsymbol{v} \cdot \nabla c^\infty) = \text{Pe}^2 \boldsymbol{v} \cdot \nabla(\boldsymbol{v} \cdot \nabla c^\infty)$, where in the second equality we have used the assumption of irrotational flow, $\nabla^2 \boldsymbol{v} = 0$. Thus,

$$\int \boldsymbol{n} c^\infty \, dS = \frac{4\pi}{3} \nabla c^\infty|_{r=0} + \frac{4\pi}{30} \text{Pe}\nabla(\boldsymbol{v} \cdot \nabla c^\infty)|_{r=0} + O(\text{Pe}^2). \quad (A8)$$

Similarly,

$$\int \boldsymbol{n}\boldsymbol{n} \nabla c^\infty \, dS = \frac{4\pi}{3} \nabla c^\infty|_{r=0} + \frac{4\pi}{10} \text{Pe}\nabla(\boldsymbol{v} \cdot \nabla c^\infty)|_{r=0}$$
$$+ O(\text{Pe}^2). \quad (A9)$$

Finally, substituting (A8) and (A9) into (A5) and using the definition of the anisotropy parameter, $\boldsymbol{A} = (4\pi)^{-1} \int c\boldsymbol{n} \, dS$, yields Eq. (1).

2. Derivation of Eq. (4)

Here we derive Eq. (4). For an isolated cell $c^\infty = 0$, so the first two terms on the right-hand side of Eq. (2) are zero. Using Eq. (3) and $c = \gamma/r$ for the isolated disturbance at Pe = 0, the integrand of the volume integral in Eq. (2) is

$$c\boldsymbol{v} \cdot \nabla \left(\frac{\boldsymbol{r}}{r^3} \right) = \frac{\gamma}{r} \left[\boldsymbol{U} \left(\frac{1}{r^3} + \frac{1}{2r^6} \right) + \boldsymbol{U} \cdot \boldsymbol{r}\boldsymbol{r} \left(\frac{3}{2r^8} - \frac{3}{r^5} \right) \right]. \quad (A10)$$

The integrand (A10) decays as $1/r^4$ at large distances: Hence, the volume integral is convergent. The integral is performed

in spherical coordinates to yield

$$\int c\boldsymbol{v} \cdot \nabla \left(\frac{\boldsymbol{r}}{r^3} \right) dV = \pi \gamma \boldsymbol{U}. \quad (A11)$$

Note that the $1/r^4$ decay of the integrand means that the contribution to the integral from the concentration disturbance in the outer region, $r = O(1/\text{Pe})$, is $O(\text{Pe})$ and thus subdominant to the $O(1)$ contribution from the inner region, $r = O(1)$. This is fortunate since the expression $c = \gamma/r$ is not valid in the outer region, where advection plays a leading-order role even though Pe is small. Finally, inserting (A11) into (2) yields (4).

3. Derivation of Eq. (6)

Consider a pair of cells separated by a distance $\boldsymbol{d}$ and oriented at an angle δ to the ambient interstitial flow (Fig. 1). The background concentration around cell 2 due to the presence of cell 1 is $c^\infty = \gamma/|\boldsymbol{r}_2 + \boldsymbol{d}|$, where $\boldsymbol{r}_2$ is the position vector measured from cell 2. Therefore,

$$\nabla c^\infty = -\gamma \frac{\boldsymbol{r}_2 + \boldsymbol{d}}{|\boldsymbol{r}_2 + \boldsymbol{d}|^3}, \quad (A12)$$

from which

$$\nabla c^\infty|_{r_2=0} = -\gamma \frac{\boldsymbol{d}}{d^3}. \quad (A13)$$

Cell 2 sits in a background velocity field $\boldsymbol{v} = \boldsymbol{U} + O(d^{-3})$, where the $O(d^{-3})$ error is due to the presence of cell 1. Therefore, we have

$$\nabla(\boldsymbol{v} \cdot \nabla c^\infty) = -\gamma \boldsymbol{U} \cdot \left[\frac{\boldsymbol{I}}{|\boldsymbol{r}_2 + \boldsymbol{d}|^3} - 3\frac{(\boldsymbol{r}_2 + \boldsymbol{d})(\boldsymbol{r}_2 + \boldsymbol{d})}{|\boldsymbol{r}_2 + \boldsymbol{d}|^5} \right]$$
$$+ O(d^{-6}), \quad (A14)$$

from which

$$\nabla(\boldsymbol{v} \cdot \nabla c^\infty)|_{r_2=0} = -\gamma \boldsymbol{U} \cdot \left(\frac{\boldsymbol{I}}{d^3} - 3\frac{\boldsymbol{d}\boldsymbol{d}}{d^5} \right) + O(d^{-6}). \quad (A15)$$

Next, we evaluate the volume integral in Eq. (2), for which we need $c - c^\infty$ from the purely diffusive (Pe = 0) concentration field. To a first approximation at large d the ligand concentration at Pe = 0 is a superposition of the sources due to each cell in isolation: $c \sim c^{(1)} + c^{(2)}$ as $d \to \infty$, where $c^{(i)} = \gamma/r_i$. The effect of cell 1 on cell 2 is evaluated using the identity [37]

$$\frac{1}{r_i^{n+1}} P_n^m(\mu_i)$$
$$= \frac{1}{R^{n+1}} \sum_{s=m}^{\infty} \frac{(n+s)!}{(s+m)!(n-m)!} \left(\frac{r_{3-i}}{R} \right)^s P_s^m[(-1)^i \mu_{3-i}], \quad (A16)$$

which enables spherical harmonics originating at cell i to be expanded in the coordinate system of cell $3 - i$, where $i = 1$ or 2. Here $\mu_i = \cos\theta_i$ and P_n^m is an associated Legendre polynomial of order m and degree n. Therefore, the ligand field secreted by cell 1 near the surface of cell 2 is

$$c^{(1)} = \frac{\gamma}{d} \left[1 - \frac{r_2}{d} P_1^0(\mu_2) + \left(\frac{r_2}{d} \right)^2 P_2^0(\mu_2) + O(d^{-3}) \right]. \quad (A17)$$

Cell 2 responds to the field (A17) by generating a function, or first reflection, $c^{(21)}$ say, which solves $\nabla^2 c^{(21)} = 0$, attenuates at large distances, and satisfies

$$\frac{\partial c^{(21)}}{\partial r_2} - \alpha c^{(21)}$$

$$= -\left[\frac{\partial c^{(1)}}{\partial r_2} - \alpha c^{(1)}\right]$$

$$= \gamma\left[\frac{\alpha}{d} + (1-\alpha)\frac{P_1^0(\mu_2)}{d^2} + (\alpha-2)\frac{P_2^0(\mu_2)}{d^3} + O(d^{-4})\right] \tag{A18}$$

at $r_2 = 1$. The latter boundary condition is derived from the flux condition at the cell surface, $-\partial c/\partial r_2 = \beta - \alpha c$, noting that the leading-order field $c^{(2)} = \gamma/r_2$, where $\gamma = \beta/(1+\alpha)$. It is readily shown that

$$c^{(21)} = \gamma\left[-\frac{\alpha}{1+\alpha}\frac{1}{d}\frac{1}{r_2} + \frac{\alpha-1}{2+\alpha}\frac{1}{d^2}\frac{P_1^0(\mu_2)}{r_2^2}\right.$$

$$\left. + \frac{2-\alpha}{3+\alpha}\frac{1}{d^3}\frac{P_2^0(\mu_2)}{r_2^3} + O(d^{-4})\right]. \tag{A19}$$

Although $c^{(21)}$ has an error of $O(d^{-4})$, to complete the calculation of the concentration around cell 2 through $O(d^3)$ we need to consider multiple reflections. Specifically, the field $c^{(21)}$ forces a harmonic reflection $c^{(121)}$ around cell 1 which satisfies the flux condition

$$\frac{\partial c^{(121)}}{\partial r_1} - \alpha c^{(121)} = -\left[\frac{\partial c^{(21)}}{\partial r_1} - \alpha c^{(21)}\right],$$

$$= -\frac{\gamma\alpha^2}{1+\alpha}\frac{1}{d^2} + O(d^{-3}). \tag{A20}$$

at $r_1 = 1$. Thus, we have

$$c^{(121)} = \frac{\gamma\alpha}{(1+\alpha)^2}\frac{1}{d^2}\frac{1}{r_1} + O(d^{-3}). \tag{A21}$$

In turn, $c^{(121)}$ forces another harmonic reflection $c^{(2121)}$ around cell 2 which satisfies the flux condition

$$\frac{\partial c^{(2121)}}{\partial r_2} - \alpha c^{(2121)} = -\left[\frac{\partial c^{(121)}}{\partial r_2} - \alpha c^{(121)}\right]$$

$$= \frac{\gamma\alpha^3}{(1+\alpha)^2}\frac{1}{d^3} + O(d^{-4}). \tag{A22}$$

at $r_2 = 1$. Thus, we have

$$c^{(2121)} = -\frac{\gamma\alpha^3}{(1+\alpha)^3}\frac{1}{d^3}\frac{1}{r_2} + O(d^{-4}). \tag{A23}$$

Therefore, from (A19) and (A23) we have the concentration disturbance around cell 2 correct through $O(d^{-3})$ given by

$$c - c^\infty$$

$$= \gamma\left[\frac{1}{r_2} - \frac{\alpha}{1+\alpha}\frac{1}{d}\frac{1}{r_2} + \frac{\alpha-1}{2+\alpha}\frac{1}{d^2}\frac{P_1^0(\mu_2)}{r_2^2}\right.$$

$$\left. + \frac{2-\alpha}{3+\alpha}\frac{1}{d^3}\frac{P_2^0(\mu_2)}{r_2^3} - \frac{\alpha^3}{(1+\alpha)^3}\frac{1}{d^3}\frac{1}{r_2} + O(d^{-4})\right]. \tag{A24}$$

Next, from (A10) we have that

$$\boldsymbol{v}\cdot\nabla\left(\frac{\boldsymbol{r}_2}{r_2^3}\right) = \left(\frac{1}{r_2^3} + \frac{1}{2r_2^6}\right)(\cos\delta\boldsymbol{e}_z - \sin\delta\boldsymbol{e}_x)$$

$$+ \left(\frac{3}{2r_2^6} - \frac{3}{r_2^3}\right)(\sin\theta_2\cos\phi\boldsymbol{e}_x$$

$$+ \sin\theta_2\sin\phi\boldsymbol{e}_y + \cos\theta_2\boldsymbol{e}_z)$$

$$(\cos\delta\cos\theta_2 - \sin\delta\sin\theta_2\cos\phi), \tag{A25}$$

in terms of spherical coordinates around cell 2. Thus, using (A24) and (A25), the volume integral in Eq. (2) is performed to spherical coordinates to yield

$$\int(c - c^\infty)\boldsymbol{v}\cdot\nabla\left(\frac{\boldsymbol{r}}{r^3}\right)dV$$

$$= \frac{\gamma\pi}{2}\left[\boldsymbol{U} - \frac{\alpha}{1+\alpha}\frac{1}{d}\boldsymbol{U} + \frac{\alpha-2}{7(\alpha+3)}\boldsymbol{U}\cdot\left(\boldsymbol{I} + \frac{\boldsymbol{dd}}{d^2}\right)\frac{1}{d^3}\right.$$

$$\left. - \frac{\alpha^3}{(1+\alpha)^3}\frac{1}{d^3}\boldsymbol{U} + O(d^{-4})\right], \tag{A26}$$

where we have used $\boldsymbol{U} = \cos\delta\boldsymbol{e}_z - \sin\delta\boldsymbol{e}_x$ and $\boldsymbol{d} = d\boldsymbol{e}_z$. Notice that there is no $O(d^{-2})$ contribution to (A26) due to the dipolar form of the concentration disturbance at this order (A24). Finally, inserting (A13), (A15), and (A26) into Eq. (2) yields Eq. (6) for the anisotropy order parameter $\boldsymbol{A}$.

---

[1] M. E. Fleury, K. C. Boardman, and M. A. Swartz, Autologous morphogen gradients by subtle interstitial flow and matrix interactions, Biophys. J. **91**, 113 (2006).

[2] J. D. Shields, M. E. Fleury, C. Yong, A. A. Tomei, G. J. Randolph, and M. A. Swartz, Autologous chemotaxis as a mechanism of tumor cell homing to Lymphatics via interstitial flow and autocrine CCR7 signaling, Cancer Cell **11**, 526 (2007).

[3] M. A. Swartz and M. E. Fleury, Interstitial flow and its effects in soft tissues, Annu. Rev. Biomed. Eng. **9**, 229 (2007).

[4] M. A. Swartz and A. W. Lund, Lymphatic and interstitial flow in the tumour microenvironment: Linking mechanobiology with immunity, Nat. Rev. Cancer **12**, 210 (2012).

[5] H. Wiig and M. A. Swartz, Interstitial fluid and lymph formation and transport: Physiological regulation and roles in inflammation and cancer, Physiol. Rev. **92**, 1005 (2012).

[6] J. M. Munson and A. C. Shieh, Interstitial fluid flow in cancer: Implications for disease progression and treatment, Cancer Manag. Res. **6**, 317 (2014).

[7] D. T. Butcher, T. Alliston, and V. M. Weaver, A tense situation: Forcing tumour progression, Nat. Rev. Cancer **9**, 108 (2009).

[8] G. Follain, D. Herrmann, S. Harlepp, V. Hyenne, N. Osmani, S. C. Warren, P. Timpson, and J. G. Goetz, Fluids and their mechanics in tumour transit: Shaping metastasis, Nat. Rev. Cancer **20**, 107 (2020).

[9] W. J. Polachek, J. L. Charest, and R. D. Kamm, Interstitial flow influences direction of tumor cell migration through competing mechanisms, Proc. Natl. Acad. Sci. U.S.A **108**, 11115 (2011).

[10] K. M. Kingsmore, D. K. Logsdon, D. H. Floyd, S. M. Peirce, B. W. Purow, and J. M. Munson, Interstitial flow differentially increases patient-derived glioblastoma stem cell invasion via CXCR4, CXCL12, and CD44-mediated mechanisms, Integr. Biol. **8**, 1246 (2016).

[11] R. Chase Cornelison, C. E. Brennan, K. M. Kingsmore, and J. M. Munson, Convective forces increase CXCR4-dependent glioblastoma cell invasion in GL261 murine model, Sci. Rep. **8**, 17057 (2018).

[12] C.-L. E. Helm, M. E. Fleury, A. H. Zisch, F. Boschetti, and M. A. Swartz, Synergy between interstitial flow and VEGF directs capillary morphogenesis in vitro through a gradient amplification mechanism, Proc. Natl. Acad. Sci. U.S.A. **102**, 15779 (2005).

[13] S. Fancher, M. Vennetilli, N. Hilgert, and A. Mugler, Precision of Flow Sensing by Self-Communicating Cells, Phys. Rev. Lett. **124**, 168101 (2020).

[14] D. Ellison, A. Mugler, M. D. Brennan, S. H. Lee. R. J. Huebner, E. R. Shamir, L. A. Woo, J. Kim, P. Amar, I. Nemenman, A. J. Ewald, and A. Levchenko, Cell-cell communication enhances the capacity of cell ensembles to sense shallow gradients during morphogenesis, Proc. Natl. Acad. Sci. U.S.A. **113**, E679 (2016).

[15] A. Mugler, A. Levchenko, and I. Nemenman, Limits to the precision of gradient sensing with spatial communication and temporal integration, Proc. Natl. Acad. Sci. U.S.A. **113**, E689 (2016).

[16] W-J. Rappel, Cell-cell communication during collective migration, Proc. Natl. Acad. Sci. U.S.A. **113**, 1471 (2016).

[17] A. Puliafito, A. De Simone, G. Seano, P. A. Gagliardi, L. Di Biasio, F. Chianale, A. Gamba, L. Primo, and A. Celani, Three-dimensional chemotaxis-driven aggregation of tumor cells, Sci. Rep. **5**, 15205 (2015).

[18] J. Varennes, S. Fancher, B. Han, and A. Mugler, Emergent Versus Individual-Based Multicellular Chemotaxis, Phys. Rev. Lett. **119**, 188101 (2017).

[19] A. C. Shieh, H. A. Rozansky, B. Hinz, and M. A. Swartz, Tumor cell invasion is promoted by interstitial flow-induced matrix priming by stromal fibroblasts, Cancer Res. **71**, 790 (2011).

[20] H. C. Brinkman, A calculation of the viscous force exerted by a flowing fluid on a dense swarm of particles, Appl. Sci. Res. **1**, 27 (1947).

[21] S. R. Chary and R. K. Jain, Direct measurement of interstitial convection and diffusion of albumin in normal and neoplastic tissues by fluorescence photobleaching, Proc. Natl. Acad. Sci. U.S.A. **86**, 5385 (1989).

[22] R. Li, J. C. Serrano, H. Xing, T. A. Lee, H. Azizgolshani, M. Zaman and R. D. Kamm, Interstitial flow promotes macrophage polarization toward an M2 phenotype, Mol. Biol. Cell **29**, 1927 (2018).

[23] S. Kim and S. J. Karrila, *Microhydrodynamics: Principles and Selected Applications* (Dover, Mineola, NY, 2005).

[24] A. M. Leshansky and A. Nir, Thermocapillary alignment of gas bubbles induced by convective transport, J. Colloid Interface Sci. **240**, 544 (2001).

[25] E. Yariv, Inertia-induced electrophoretic interactions, Phys. Fluids **16**, L24 (2004).

[26] A. S. Khair, Diffusiophoresis of colloidal particles in neutral solute gradients at finite Péclet number, J. Fluid Mech. **731**, 64 (2013).

[27] A. Acrivos and T. Taylor, Heat and mass transfer from single spheres in Stokes flow, Phys. Fluids **5**, 387 (1962).

[28] H. Brenner, Forced convection heat and mass transfer at small Péclet numbers from a particle of arbitrary shape, Chem. Eng. Sci. **18**, 109 (1963).

[29] H. Masoud and H. A. Stone, The reciprocal theorem in fluid dynamics and transport phenomena, J. Fluid Mech. **879**, P1 (2019).

[30] J. O. Waldeland and S. Evje, A multiphase model for exploring tumor cell migration driven by autologous chemotaxis, Chem. Eng. Sci. **191**, 268 (2018).

[31] A. Li and R. Sun, Role of interstitial flow in tumor migration through 3D ECM, Acta Mech. Sin. **36**, 768 (2020).

[32] G. S. Rosalem, E. B. L. Casas, T. P. Lima, and L. Andrés González-Torres, A mechanobiological model to study upstream cell migration guided by tensotaxis, Biomech. Model. Mechanobiol. **19**, 1537 (2020).

[33] D. K. Ross, The potential due to two point charges each at the centre of a spherical cavity and embedded in a dielectric medium, Aust. J. Phys. **21**, 817 (1968).

[34] G. B. Jeffery, On a form of the solution of Laplace's equation suitable for problems relating to two spheres, Proc. R. Soc. Lond. A **87**, 109 (1912).

[35] A. Acrivos, E. J. Hinch, and D. J. Jeffrey, Heat transfer to a slowly moving fluid from a dilute fixed bed of heated spheres, J. Fluid Mech. **101**, 403 (1980).

[36] J. F. Morris and J. F. Brady, Bulk reaction rate in a heterogeneous reaction system, Ind. Eng. Chem. Res. **34**, 3514 (1995).

[37] D. J. Jeffrey, Conduction through a random suspension of spheres, Proc. R. Soc. Lond. A **335**, 355 (1973).